中国激光

焊点形状对GH3230高温合金激光焊接性能的影响

许璠[1*]，李星[2]，刘政[1]，薄佑锋[1]，陈昆宇[1]

[1]西安航天发动机有限公司，陕西 西安 710100；

[2]航天推进技术研究院，陕西 西安 710100

摘要 为进一步提高冲压发动机火焰筒基体与加强环之间的焊接强度，考虑产品的实际结构，设计了4种不同形状的焊点，即环形、C形、椭圆形和S形焊点，对比研究了这4种焊点的性能差异。首先采用激光焊接方法对GH3230高温合金薄板进行搭接焊接试验，然后比较4种焊点在焊缝成形、力学性能、断裂行为以及微观组织方面的差异，最终确定了最优的焊接方案。结果表明：当搭接区域的面积一定时，新提出的S形焊点因为具有焊接熔合面面积大、焊缝不闭合留有应力释放区等优点，抗剪性能更优且焊缝成形质量良好；S形焊点焊缝的抗剪强度为原环形焊点焊缝的1.8倍，适合用于火焰筒等薄壁类产品的焊接。

关键词 激光技术；焊点形状；薄壁零件；焊接强度；高温合金GH3230

中图分类号 TG456.7 **文献标志码** A **DOI**：10.3788/CJL211526

1 引 言

液体冲压发动机具有推重比高、结构简单以及质量轻等特点，是高动态临近空间飞行器的理想动力装置，世界各军事大国都在大力发展冲压发动机技术[1]。在大流量加严试车考核中，某型号冲压发动机燃烧室火焰筒基体与加强环之间出现了焊点脱落现象，确定此处为该型号发动机的薄弱环节。发动机上的火焰筒与加强环材料均为高温合金GH3230，前期两者的焊接方法为电阻点焊，后考虑到激光焊具有能量密度高、焊接速度快、接头质量高等优点[2-7]，改为激光焊工艺，但仍存在焊缝撕裂的风险。为了进一步提高火焰筒与加强环结构的承载能力和服役寿命，需要对高温合金薄板构件的焊接工艺进行进一步研究[8-10]。

目前，国内外学者对激光焊接进行了大量研究：Daneshpour等[11-12]在研究厚度为2 mm的先进高强度钢DP780的激光点焊时，提出了激光环形焊点的概念，并认为激光焊点的疲劳性能不低于电阻焊点的疲劳性能，且激光焊点周边有更大的压应力区，可以延缓裂纹扩展并提高焊点的承载力。Torkamany等[13]对0.8 mm低碳钢/奥氏体不锈钢薄板进行了激光环形点焊，研究了激光功率对搭接焊点性能的影响，并发现提高激光功率会显著增大下层板的熔合区尺寸，继而提高焊点的抗剪强度。吕涛等[14]研究了焊点形状不同的厚度为1.5 mm的TC4钛合金板材的抗剪性能差异，揭示了焊点的抗剪性能与熔合面面积有关，且两者呈正相关关系。刘春艳等[15]开展了环形焊点和C形焊点的对比研究，试件为1 mm厚GH99镍基高温合金平板；结果显示，C形焊点的焊后应力及变形更小。他们认为，环形焊缝为闭合曲线，不利于应力释放，而C形焊缝不闭合，应力可在一定程度上得以释放，所以C形焊缝较环形焊缝具有更好的焊接质量。针对厚度在0.2 mm以下的薄片材料的焊接，周常多[16]提出了一种弓字形非闭合的激光扫描路径及激光焊接方法，并实现不锈钢薄片的焊接，获得了拉力大的焊点。张伟[17]探究了激光束路径对1 mm厚第三代高强钢DP980接头性能的影响，分析了不同接头的断裂过程及断裂机制，认为焊接接头拉应力、剪应力之间的竞争是导致不同断裂行为的主要因素。

从以上的研究可以看出，激光焊点形状近年来已成为一个新的研究热点，对焊点形状进行优化可以有效提高焊接强度和焊接质量，但目前的研究还存在一些问题：1）随着火焰筒产品设计指标的进一步提高，现有的焊点形状难以满足更加严苛条件下的高强度考核要求，环形、C形等形状的焊点仍存在失效的风险；2）部分已有的焊点形状不适用于厚度约为1 mm高温合金薄板搭接结构，而且有关焊点形状对该类搭接结构焊接性能影响的研究还较少。为此，本团队在之前研究的基础上，对火焰筒与加强环之间的焊点形状进行重新设计，比较了环形、C形、椭圆形以及S形焊点在焊缝成形质量、拉伸性能、组织以及断裂特征等方面的差异，确定了最优的焊接方案，为冲压发动机的实际焊接提供参考依据。

收稿日期：2021-11-15；**修回日期**：2022-01-05；**录用日期**：2022-05-07；**网络首发日期**：2022-05-20

通信作者：*xfan710100@163.com

2　试验方案与分析方法

2.1　焊点形状设计

考虑到产品的实际结构，在原来环形焊点、C形焊点[14-15]的基础上，本团队新设计了增加长度的椭圆形和适应产品结构特点的S形焊点。同时，由于火焰筒波纹与加强环在中心处贴合较好而在边缘处贴合较差，搭接区域的有效焊接范围为8 mm×4 mm，因此，本团队在此区域内设计焊点形状，确定焊点的尺寸。4种形状的焊点如图1所示。

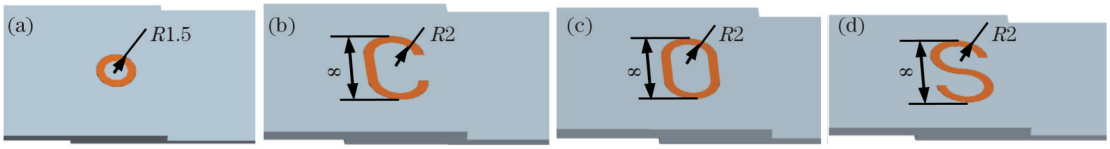

图1　4种形状的焊点。(a)环形焊点；(b)C形焊点；(c)椭圆形焊点；(d)S形焊点

Fig. 1　Four shapes of welding spot. (a) Ring-welding spot; (b) C-welding spot; (c) oval-welding spot; (d) S-welding spot

图1(a)为环形焊点，其长度为9.42 mm，为原路线方案。图1(b)是根据参考文献设计的C形焊点，其长度为16.56 mm(长度约为原路线的1.76倍)，该路线是不封闭曲线，留出了应力释放区。图1(c)是椭圆形焊点，其长度为20.56 mm(长度为原路线的2.18倍)。图1(d)是S形焊点，其长度为18.84 mm(长度为原路线的2倍)；该形状焊点既留出了应力释放区，又增加了焊缝路线长度，而且焊缝较椭圆形焊点更靠近搭接区域中心，避免了焊缝位于搭接区域的边缘，但边缘处两板的间隙较大，会影响焊接质量。

2.2　试验材料及分析方法

试验用材料为Ni-Cr基固溶强化型变形高温合金GH3230，其主要化学成分和物理性能如表1和图2所示。试板经过了标准热处理，其尺寸为100 mm×20 mm，板Ⅰ的厚度为1 mm，板Ⅱ的厚度为0.6 mm，接头形式为搭接，搭接区域的宽度为12 mm。

焊接设备为UPRB4600型激光焊机，光纤激光器的最大输出功率为2 kW，最小聚焦光斑直径为0.3 mm，焦距为200 mm。焊接前，先用丙酮清洁试件表面，去除其表面的油垢等。焊接时，采用单面焊接一次成形，试件正面、背面均采用纯度为99.99%的氩气进行保护，保护气体的流量分别为20 L/min和10 L/min，固定离焦量为0 mm。焊接工艺参数见表2，每种参数下焊接3个试件。线能量由激光功率除以焊接速度得到，计算每种参数下的线能量。焊后，采用VHX-600K超景深数码光学显微镜观察接头横截面的微观组织，采用Instron-5569万能试验机对接头进行拉伸-剪切测试，采用Hitachi S-4700扫描电镜(SEM)观察焊点的断裂方式。

表1　GH3230高温合金的化学成分

Table 1　Chemical composition of GH3230 superalloy

Element	Mass fraction/%
C	0.05 – 0.15
Cr	20.00 – 24.00
Ni	Bal.
Co	≤5.00
W	13.00 – 15.00
Mo	1.00 – 3.00
Al	0.20 – 0.50
Ti	≤0.10
Fe	≤3.00
La	0.005 – 0.05
B	≤0.015
Si	0.25 – 0.75
Mn	0.30 – 1.00
S	≤0.015
P	≤0.03
Cu	≤0.50

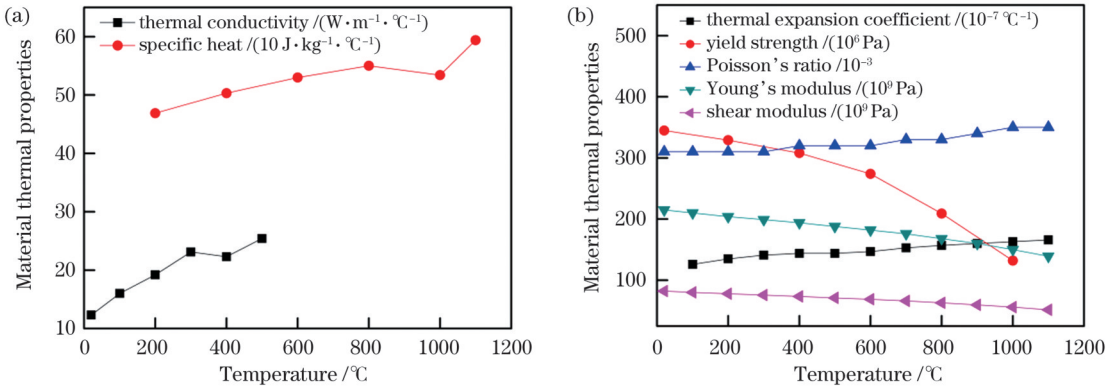

图2　GH3230的材料特性。(a)热物理性能；(b)力学性能

Fig. 2　Material properties of GH3230. (a) Thermophysical properties; (b) mechanical properties

表 2　激光焊接工艺参数

Table 2　Parameters of laser welding

No.	Laser power Q/kW	Welding speed v/(mm•s^{-1})	Linear energy E/(J•mm^{-1})	Welding spot shape
1	0.7	20	37	S-welding spot
2	0.7	30	24.7	S-welding spot
3	0.7	40	18.5	S-welding spot
4	1.0	20	50	S-welding spot
5	1.0	30	33.3	S-welding spot
6	1.0	40	25	S-welding spot
7	1.4	20	70	S-welding spot
8	1.4	30	46.7	S-welding spot
9	1.4	40	35	S-welding spot
10	0.7	20	37	Oval-welding spot
11	1.4	40	35	Oval-welding spot
12	1.4	40	35	Ring-welding spot
13	0.7	20	37	C-welding spot
14	1.4	40	35	C-welding spot

3　试验结果与讨论

3.1　焊后形貌特征

图 3 为优化工艺参数[18]后的环形、椭圆形、C 形以及 S 形焊点的表面形貌及横截面形貌，其中第一、二行图分别为焊点的正面、背面形貌，第三行图为焊点的横截面形貌，横截面的位置如金相图左下角处焊点形状二维图中的剖切符号所示。由图 3 可知，4 种焊点均可获得较好的焊缝成形质量，焊点表面光滑无飞溅，稍有一定的氧化，焊缝均已焊透，无气孔、裂纹等缺陷。

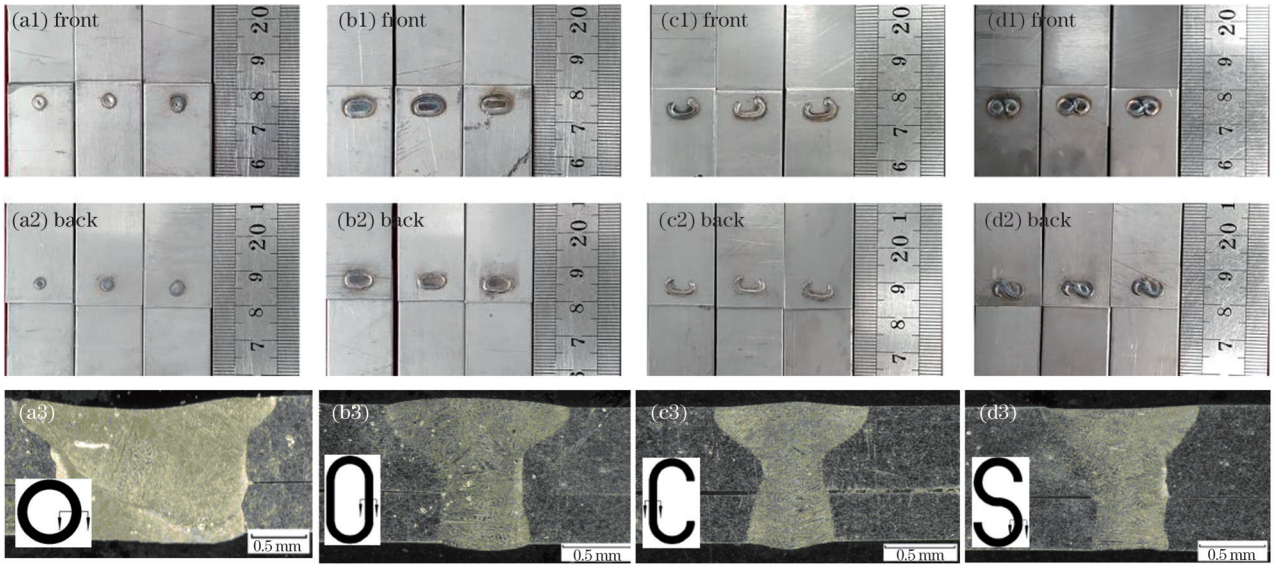

图 3　焊点表面及横截面形貌。(a)环形焊点；(b)椭圆形焊点；(c)C 形焊点；(d)S 形焊点

Fig.3　Surface and cross-section morphologies of laser welding spots. (a) Ring-welding spot; (b) oval-welding spot; (c) C-welding spot; (d) S-welding spot

对于 S 形焊点，焊缝熔宽与线能量之间的关系如图 4 所示。对试验数据进行拟合，可获得焊缝熔宽与线能量之间的函数关系式，即

$$D_{top}=0.025E+0.683, \tag{1}$$

$$D_{back}=0.054E-1.022, \tag{2}$$

式中：D_{top} 为表面熔宽；D_{back} 为背面熔宽；E 为线能量。根据式(1)和式(2)，可预测不同焊接参数下的焊缝成形情况。线能量输入不宜过大，否则会引起热裂纹和烧穿等缺陷。

由图 4 和式(1)、(2)可以发现，随着线能量增加，焊缝的表面熔宽和背面熔宽均增加，且背面熔宽的增加幅度更大。这是因为在焊接时，随着线能量增大，熔池体积与总熔化金属量相应增大，焊缝熔宽增加，而且由于熔池的小孔效应增强，小孔里面的金属蒸气会先

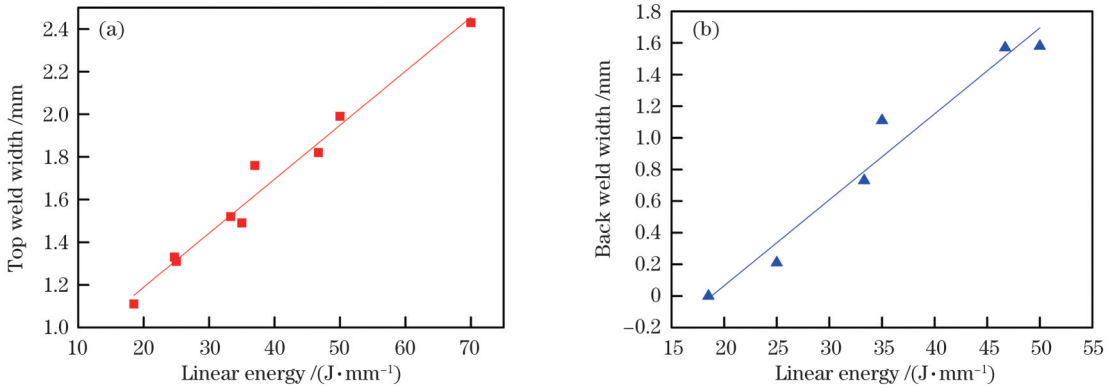

图 4　线能量对焊缝熔宽的影响。(a)表面熔宽;(b)背面熔宽

Fig. 4　Effect of linear energy on weld width. (a) Top weld width; (b) back weld width

从焊缝背面逸出,背面接收的激光能量增加,所以焊缝背面熔宽的增幅更大。

3.2　力学性能

采用万能试验机对 4 种接头进行拉伸-剪切测试,每组测试三次,拉伸方向如图 5 所示。计算三次测试的平均值,结果如图 6 所示。激光功率为 1.4 kW 和 0.7 kW 时,C 形焊点的拉断力分别为 5576.3、5308.3 N,椭圆形焊点的拉断力分别为 6802、6415.3 N,S 形焊点的拉断力分别为 6901.3、6305.6 N,环形焊点的拉断力为 3843 N(此值对应的是 1.4 kW 激光功率)。可以发现,S 形焊点、椭圆形焊点的拉断力较大,C 形焊点的次之,环形焊点的最小。这表明,在一定条件下,焊点的几何长度越大,其抗剪性能越好。因此,S 形焊点和椭圆形焊点更适合拉断力要求较高的结构。

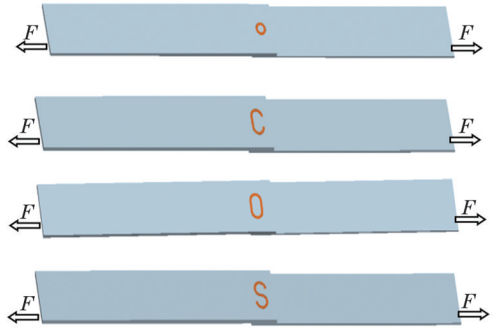

图 5　试样的拉伸方向

Fig. 5　Tensile direction of samples

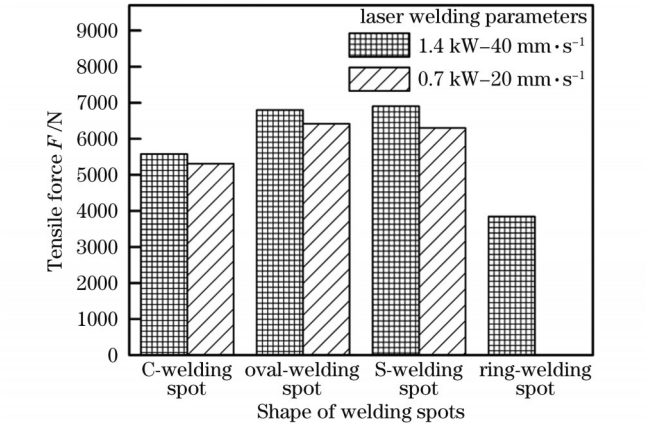

图 6　不同形状焊点的拉断力对比

Fig. 6　Tensile force comparison of different shapes of welding spots

采用焊点的轨迹长度乘以线能量,计算 4 种焊点获得的总能量,计算结果如图 7 所示。可以看出,椭圆形焊点、S 形焊点获得的能量较大,C 形焊点次之,环形焊点最小。这说明在一定条件下,焊点的几何长度越长,获得的能量越大,抗剪性能越好。但是,椭圆形焊点为封闭曲线,焊接时拘束度大,焊后极易产生变形和裂纹,会降低抗剪性能;而 S 形焊点为不闭合曲线,应力可以在一定程度上释放,不易产生缺陷。所以,S 形焊点的性能较椭圆形焊点更好。

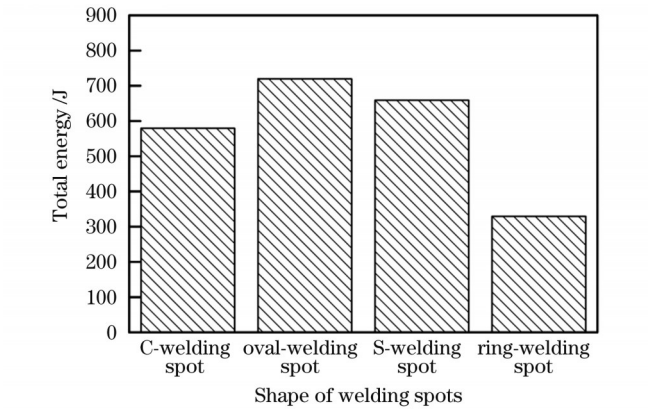

图 7　不同形状焊点的激光总能量对比

Fig. 7　Total laser energy comparison of different shapes of welding spots

换算得到了不同形状焊点的焊缝在单位长度上承受的拉断力,如图 8 所示。由图 8 可知,S 形焊点的焊缝在单位长度上承受的拉断力最大,C 形焊点的焊缝次之,椭圆形焊点的焊缝最小。这表明 S 形焊点的焊缝质量最优,可以在单位长度上承受更大的拉断力。

对于 S 形焊点,测量不同工艺参数下接头的拉断力,测量结果如表 3 所示,拉断力在 3467.7~7112.7 N 之间。由 1#、4#、7#参数下的测试结果可以看出,随着激光功率增加,接头的拉断力逐渐增大;由 4#、5#、6#参

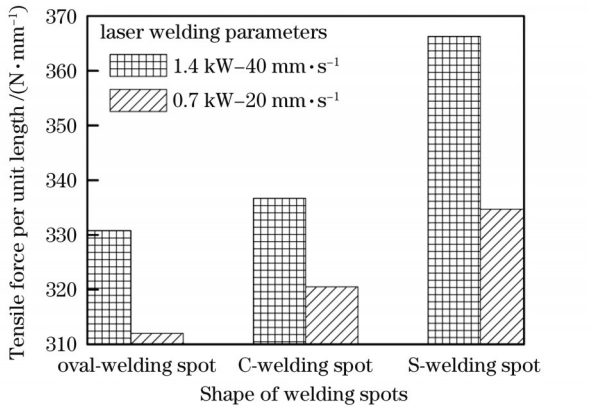

图 8　单位长度焊缝的拉断力对比

Fig. 8　Comparison of tensile force per unit length

数下的测试结果可以看出，随着焊接速度增大，接头的拉断力逐渐降低。上述工艺参数下接头的载荷曲线如图 9 所示。

表 3　不同参数下的 S 形焊点的拉断力测试结果

Table 3　Tensile force of S-welding spot welded under different parameters

No.	Laser power / kW	Welding speed / (mm•s^{-1})	Force/N
1	0.7	20	6305.6
2	0.7	30	4779.7
3	0.7	40	3467.7
4	1.0	20	6975.3
5	1.0	30	6281.0
6	1.0	40	6148.3
7	1.4	20	7073.5(crack and hole)
8	1.4	30	7112.7
9	1.4	40	6901.3

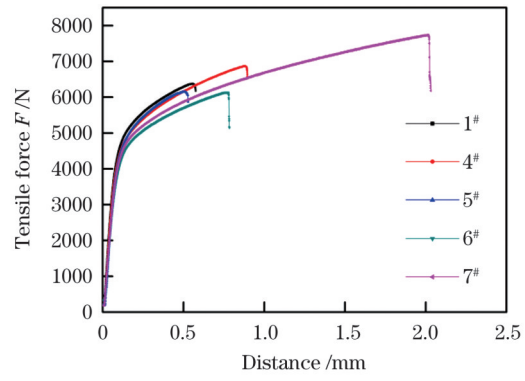

图 9　不同工艺参数下接头的拉断力曲线

Fig. 9　Tensile force curves of joint at different parameters

S 形焊点在上述参数下的熔合面宽度与接头拉断力的关系如图 10 所示。可以看出，随着熔合面宽度增加，接头所能承受的拉断力增加，而且当熔合面宽度较小时，这种增加趋势十分显著，当熔合面宽度达到 0.8 mm 后拉断力的增长放缓。

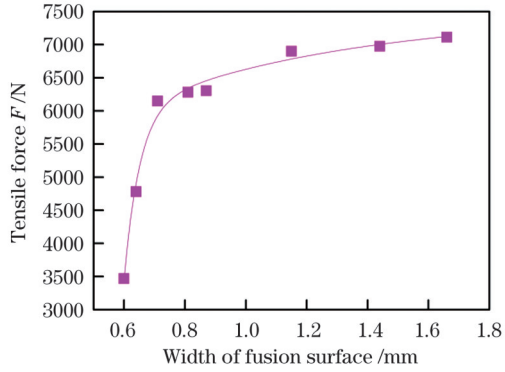

图 10　熔合面宽度与接头拉断力之间的关系

Fig. 10　Relationship between width of fusion surface and tensile force

3.3　焊点断裂行为

4 种焊点的断裂方式存在差异，如图 11 所示。从宏观形貌可以看出：1）环形焊点与 C 形焊点断裂时上下板完全分离，沿着配合面上的焊缝拉断，发生界面断裂，断裂后母材基本未受影响。这说明这两种焊点的强度远低于母材强度。2）椭圆形焊点和 S 形焊点沿着熔合线开裂，继而扩展到母材，并将母材完全拉断，发生焊缝撕裂，断裂处母材变形严重。这说明椭圆形焊点与 S 形焊点的强度与母材强度相近。

为了明晰焊点的断裂机理，分别对其进行断口扫描。4 种断口均呈韧窝状，但环形焊点、C 形焊点的韧窝较浅，且呈剪切韧窝状，说明断口承受的是剪切应力；椭圆形焊点、S 形焊点的韧窝较深，且断口边缘有显著的塑性变形，说明焊点受到的是拉剪混合应力。

比较 4 种焊点的激光总能量，分析总能量对断裂模式的影响。由图 7 及图 11 可以看出，随着激光总能量增大，断裂行为由界面断裂模式向焊缝撕裂模式转变：环形焊点与 C 形焊点的总能量分别为 329.7 J 和 579.6 J，接头呈现界面断裂模式；S 形焊点与椭圆形焊点的总能量分别为 659.4 J 和 719.6 J，接头呈现焊缝撕裂模式。综上，激光总能量会影响焊点的强度与应力状态，从而导致焊点的断裂行为不同。

3.4　组织形貌

对环形、椭圆形、C 形以及 S 形焊点进行组织分析[19]，分析结果如图 12 所示。可见，4 种焊点组织并无明显差别：焊缝区均主要为柱状晶，其生长方向大部分沿散热最快的方向；热影响区的组织均未见明显长大和晶间液化现象；晶粒度均与基体组织一样，为 6～7 级；碳化物分布均匀（表明激光焊接热输入适宜）。如前述可知，4 种焊点的激光焊接参数相同，但焊点形状不同，焊点所获得的激光总能量不同，说明这 4 种焊点的组织形貌主要与激光焊接参数有关，受焊点形状的影响不大。

综上分析，S 形焊点具有焊接熔合面大、焊缝不闭合留有应力释放区等优点，所以其力学性能优良、组织

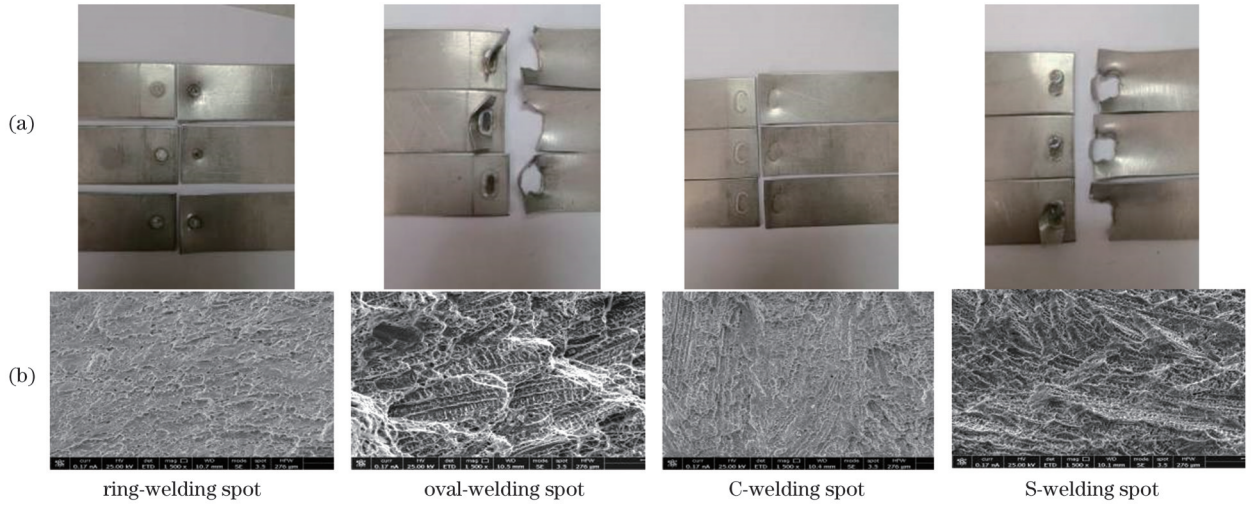

图 11　4 种焊点拉伸试样的断口形貌。(a)宏观形貌;(b)微观形貌

Fig.11　Fracture morphologies of tensile samples with four shapes of welding spots. (a) Macro-morphologies; (b) micro-morphologies

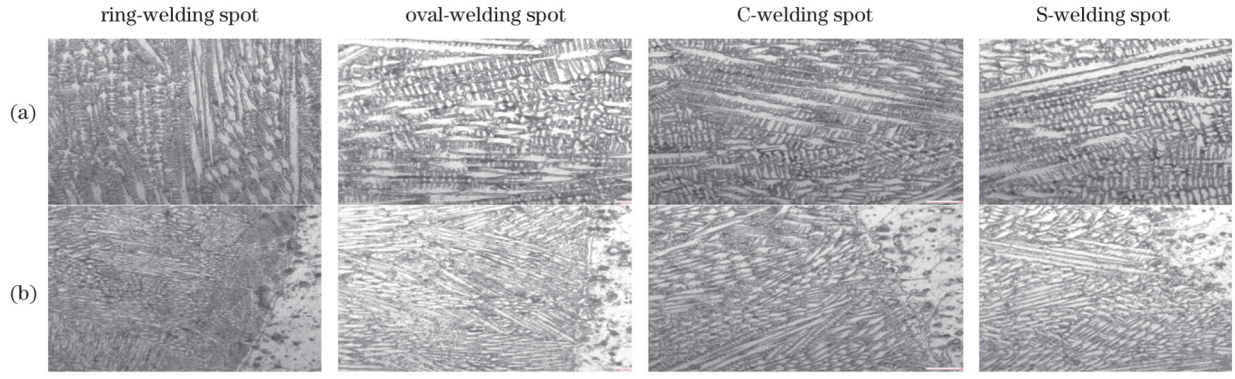

图 12　4 种焊点的显微组织。(a)焊缝区;(b)热影响区

Fig.12　Microstructures of four welding spots. (a) Weld zone; (b) heat affected zone

致密。故推荐在实际焊接时采用S形焊点。采用S形焊点进行火焰筒产品的焊接,焊缝质量合格,可以满足产品设计技术要求,焊缝的抗剪强度是原环形焊缝的1.8倍。

4　结　　论

针对薄壁搭接结构焊接强度不足这一难题,设计了4种不同形状的焊点,通过激光焊接试验,比较了不同焊点在焊缝形貌、力学性能、断裂行为等方面的差异,最终得出了以下结论:

1)采用环形、C形、椭圆形和S形焊点对GH3230高温合金进行搭接焊,焊缝在外观形貌、微观组织上的工艺适应性较好。焊缝熔宽随着热输入的增大而增加,且背面熔宽的增幅更大。

2)焊点的抗剪性能与熔合面面积有关,且随着熔合面面积的增加而增加。S形和椭圆形焊点的焊接强度最高,C形焊点的次之,环形焊点最差。环形和C形焊点的断裂方式为界面断裂,椭圆形和S形焊点的断裂方式为焊缝撕裂。

3)当搭接区域的面积一定时,S形焊点的焊接综合性能更优。S形焊点焊缝的抗剪强度是原环形焊缝的1.8倍,适合用于对焊接强度要求高的火焰筒等薄壁类产品的焊接。

参　考　文　献

[1] 徐旭, 陈兵, 徐大军. 冲压发动机原理及技术[M]. 北京: 北京航空航天大学出版社, 2014.
Xu X, Chen B, Xu D J. Ramjet principle and technology[M]. Beijing: Beijing University of Aeronautics & Astronautics Press, 2014.

[2] Mei L F, Yan D B, Chen G Y, et al. Comparative study on CO_2 laser overlap welding and resistance spot welding for automotive body in white[J]. Materials & Design, 2015, 78: 107-117.

[3] Rojhirunsakool T, Sirivedin K. Investigation of welding speed parameters on Ni-base superalloy by laser welding process[J]. Key Engineering Materials, 2020, 856: 85-91.

[4] 陈锡源, 陈俐, 常明, 等. SP700钛合金激光焊的焊缝成形与性能分析[J]. 焊接学报, 2018, 39(6): 121-125, 134.
Chen X Y, Chen L, Chang M, et al. Study on weld shaping and joint properties for SP700 titanium alloy of laser welding[J]. Transactions of the China Welding Institution, 2018, 39(6): 121-125, 134.

[5] Chen G Y, Mei L F, Zhang M J, et al. Research on key influence factors of laser overlap welding of automobile body galvanized steel [J]. Optics & Laser Technology, 2013, 45: 726-733.

[6] Reisgen U, Olschok S, Jakobs S, et al. Laser beam welding under vacuum of high grade materials[J]. Welding in the World, 2016, 60 (3): 403-413.

[7] 李龙, 李辉, 徐梅, 等. 热输入对超高强钢DP1000激光焊接接头微观组织和断裂机制的影响[J]. 焊接学报, 2018, 39(7): 75-80, 132.
Li L, Li H, Xu M, et al. Effect of heat input on microstructure and fracture mechanism of ultra high strength DP1000 steel laser welded joint[J]. Transactions of the China Welding Institution, 2018, 39(7): 75-80, 132.

[8] 玉昆. GH3535合金激光焊接头组织性能演变及腐蚀行为研究[D]. 上海: 中国科学院上海应用物理研究所, 2018: 39-45.
Yu K. Microstructure and mechanical properties evolution and corrosion behavior of laser welds in GH3535 alloy[D]. Shanghai: Shanghai Institute of Applied Physics, Chinese Academy of Sciences, 2018: 39-45.

[9] 王晓光, 刘奋成, 周宝升. GH3044合金激光焊接接头组织和变形均匀性[J]. 中国有色金属学报, 2019, 29(11): 2549-2560.
Wang X G, Liu F C, Zhou B S. Microstructure and deformation uniformity of GH3044 alloy joints by laser beam welding[J]. The Chinese Journal of Nonferrous Metals, 2019, 29(11): 2549-2560.

[10] 孙文君, 王善林, 谭观华, 等. 材料状态对GH4169高温合金激光焊接头组织与性能的影响[J]. 中国激光, 2020, 47(10): 1002006.
Sun W J, Wang S L, Tan G H, et al. Effect of material states on microstructure and properties of GH4169 superalloy laser-welded joint[J]. Chinese Journal of Lasers, 2020, 47(10): 1002006.

[11] Daneshpour S, Riekehr S, Koçak M, et al. Mechanical and fatigue behavior of laser and resistance spot welds in advanced high strength steels[J]. Science and Technology of Welding and Joining, 2009, 14(1): 20-25.

[12] Martinson P, Daneshpour S, Koçak M, et al. Residual stress analysis of laser spot welding of steel sheets[J]. Materials & Design, 2009, 30(9): 3351-3359.

[13] Torkamany M J, Sabbaghzadeh J, Hamedi M J. Effect of laser welding mode on the microstructure and mechanical performance of dissimilar laser spot welds between low carbon and austenitic stainless steels[J]. Materials & Design, 2012, 34: 666-672.

[14] 吕涛, 雷正龙, 陈彦宾, 等. 焊点形状对TC4钛合金激光点焊力学性能的影响[J]. 中国激光, 2013, 40(12): 1203002.
Lü T, Lei Z L, Chen Y B, et al. Influence of different shapes on the mechanical properties of laser spot weld of TC4 titanium alloy [J]. Chinese Journal of Lasers, 2013, 40(12): 1203002.

[15] 刘春艳, 马瑞, 檀财旺, 等. GH99高温合金环形和C形激光焊接对比研究[J]. 中国激光, 2014, 41(8): 0803002.
Liu C Y, Ma R, Tan C W, et al. Comparison of ring-form and C-form laser welding for GH99 superalloy[J]. Chinese Journal of Lasers, 2014, 41(8): 0803002.

[16] 周常多. 一种激光焊接点的激光路径及激光焊接方法: CN108356414B[P]. 2020-01-24.
Zhou C D. Laser path of laser welding point, and laser welding method: CN108356414B[P]. 2020-01-24.

[17] 张伟. 第三代高强钢激光点焊接头成形机理及断裂行为研究[D]. 长春: 中国科学院长春光学精密机械与物理研究所, 2021: 107-109.
Zhang W. Formation mechanism and fracture behavior of laser spot welded third generation high-strength steel[D]. Changchun: Changchun Institute of Optics, Fine Mechanics and Physics, Chinese Academy of Sciences, 2021: 107-109.

[18] 陈素明, 赵安安, 姜毅, 等. TC4钛合金激光填丝焊工艺参数对焊缝宏观成形的影响[J]. 中国激光, 2021, 48(14): 1402007.
Chen S M, Zhao A A, Jiang Y, et al. Influence of the technological parameters of TC4 titanium alloy laser wire filling welding on weld seam macroformation[J]. Chinese Journal of Lasers, 2021, 48(14): 1402007.

[19] 陈志伟, 马程远, 陈波, 等. 激光-MIG复合焊接中厚度不锈钢组织及性能研究[J]. 激光与光电子学进展, 2020, 57(23): 231405.
Chen Z W, Ma C Y, Chen B, et al. Microstructure and properties of medium-thick stainless steel by laser-MIG hybrid welding[J]. Laser & Optoelectronics Progress, 2020, 57(23): 231405.

Influence of Welding Spot Shapes on Laser Welding Performance of GH3230 Superalloy

Xu Fan[1*], Li Xing[2], Liu Zheng[1], Bo Youfeng[1], Chen Kunyu[1]

[1]*Xi'an Space Engine Company Limited, Xi'an* 710100, *Shaanxi, China*;

[2]*Academy of Aerospace Propulsion Technology, Xi'an* 710100, *Shaanxi, China*

Abstract

Objective Liquid ramjet is the optimum power device for high-dynamic near-space vehicles because of its high thrust-weight ratio, simple structure, and lightweight. Ramjet technology is being extensively developed by the military around the world. However, during a rigorous test, the welding spots between the flame tube and reinforcement ring of a ramjet, which was identified as the weak link, were damaged. The flame tube and strengthening ring are both made of GH3230 superalloy. First, resistance spot welding is used to weld the two parts. Moreover, laser welding was chosen as the welding method because of its high energy density, fast welding speed, and excellent welding quality. However, there is still the possibility of weld tearing between the two parts. Currently, the shape of the laser welding spot is a popular study area, and optimizing it can significantly increase welding strength and quality. Thus far, several researchers have proposed various welding shapes, such as ring- and C-welding spots. It was found that the shear performance of welding spots has a positive connection with the area of fusion surfaces. Furthermore, the ring-welding spot welding path is considered a closed curve, which is unfavorable to stress release. The C-welding spot welding path is open and can release stress; thus, it is superior to the ring-welding spot. However, the existing weld shapes still have insufficient welding strength, which reduces the reliability and assembly precision of the products. Therefore, four weld shapes, such as ring-, C-, oval-, and S-welding spots, were designed based on the real structure of the product. The differences in performance between the welding spots were compared to determine the best welding scheme. This study can be used as a reference for welding ramjet products, and it has both innovative and practical values.

Methods Laser welding experimental research was conducted for lap welding of GH3230 superalloy sheets. The differences in the weld formation, mechanical properties, fracture behavior, and microstructure of the welding spots were compared. The thickness of plate Ⅰ, the thickness of plate Ⅱ, and the width of the overlap region were 1, 0.6, and 12 mm, respectively. The welding equipment is a UPRB4600 laser welding machine, which is equipped with a 2 kW fiber laser system. During welding, a single pass was performed; the defocusing distance was set to 0 mm and three specimens were welded for every process parameter. After welding, the microstructure of the weld joint was observed using a digital optical microscope; the welding strength was tested using a universal testing machine, and the fracture morphologies was analyzed using a scanning electron microscope.

Results and Discussions Four weld shapes were designed when the overlap zone was certain: ring-, C-, oval-, and S-welding spots (Fig. 1). The differences in the weld formation, mechanical properties, fracture behavior, and microstructure of the welding spots were compared, and the following results were obtained: 1) four weld shapes showed significant adaptability in the weld formation and microstructure (Fig. 3 and Fig. 12). The weld width increased as the heat input increased, and the increase in the back weld width was greater than that of the top weld width (Fig. 4). 2) The shear performance of the welding spots was related to the area of the fusion surface, which increased as the fusion area increased. The S- and oval- welding spots had higher welding strength followed by the C- and ring-welding spots (Fig. 6). In the ring- and C-welding spots fracture modes, the weld departed from the interface, and the weld broke along the cross-section of the oval- and S-welding spots (Fig. 11). 3) The S-welding spot showed the best performance among four welding spots when the overlap zone was certain because of its geometric shape. The product of the flame tube was welded using the S-welding spot, resulting in a good welding quality. The welding strength of the S-welding spot was 1.8 times stronger than that of the ring-welding spot. Other thin-wall products that require high welding strength can benefit from the S-welding spot.

Conclusions Herein, the effects of four welding spots shapes on welding properties were studied and the optimal welding scheme was determined. The results show that the S-welding spot has better tensile-shear performance and weld formation when the overlap zone is certain because it has a large welding area, and the welding path is open, thus releasing stress. The tensile-shear strength of the improved weld is 1.8 times stronger than that of the original welding spot (C-welding spot). The S-welding spot is suitable for welding thin-wall products, such as flame tubes.

Key words laser technique; welding spot shape; thin-wall parts; welding strength; superalloy GH3230